



Study of Magnetic Symmetrical Moment of CeO₂ and its Applications

R. Rajendran¹, M. S. Dheenadayalan^{2*}

¹Research and Development Centre, Bharathiyar University, Coimbatore, 641 046, India

^{2*}Research Department of Chemistry, G.T.N Arts College, Dindigul, India

Corresponding author email id: dheenadayalanchemistry@gtnartscollege.ac.in

Abstract

Magnetic materials play the main role in recent research. The magnetic materials are used in the water treatment magnetic brake system. Super paramagnetic materials play the main role in space onstruction and a variety of applications. So the study of the magnetic nature of transitions metals gets importance in recent years. CeO₂ nanoparticle was prepared by using Ultrasonication method. X-ray diffraction is used to identify the exact grain size and crystal arrangement. (111), (022) the hkl value proves the sample purity. Scanning electron microscopy is used to identify the size and morphology of the particles. The current study explains the magnetic nature of CeO₂ by using magnetic (Daniel B.Litvin) symmetry which is identified by XRD and crystal impact Match-2 and Diamond-3 software. It proves the G-type anti ferromagnetic structure with $fm\bar{3}m$ symmetry.

Key words: Diamond-3, symmetry, group theory, CeO₂, magnetic nanoparticle.

Introduction

Numerous applications, including electrical, electronic, catalytic, adsorption, optical, electrochemical, batteries, functional materials, energy storage, magnetic data storage, and sensing properties, have been investigated for cerium oxide with various valence states and crystalline structures [1–5]. However, it is necessary to decrease the particle size and increase the active surface area of nanomaterials in order to improve various features and meet the growing demands for diverse applications. Reduced particle size improves non-conductivity, material's electrical, sensing, and catalytic characteristics [6–8]. From room temperature up to its melting point (2700°C), ceria (CeO₂), a cubic fluorite-type structured ceramic material, exhibits no known crystallographic change [9]. The majority of applications call for the use of nonagglomerated nanoparticles since aggregated nanoparticles has poor sinterability and inefficient mixing. There has been a lot of interest in improving catalytic activity, sinterability,

and other properties by shrinking the grain size into the nanometer range in recent years because of the excellent physical and chemical properties of nano-sized particles, which are very different from those of bulk particles [10, 11]. The quantity of functional Ce⁴⁺/Ce³⁺ sites and their capacity for oxygen exchange are two notable characteristics of CeO₂ [12,13]. Different methods, including hydrothermal [14], mechanochemical [15], sonochemical [16], combustion synthesis [17], sol-gel [18], semi-batch reactor [19], microemulsion [20], and spray-pyrolysis [21], have been reported to generate CeO₂ nanopowders. Precipitation is one of the more simple, economic, and time-efficient chemical reactions compared to other methods. When compared to other chemical processes, the precipitation approach is straightforward, inexpensive, and time-saving and alternative methods. In this paper, we concentrated on CeO₂ nanoparticles are created through co-precipitation. This study's objective was to create cerium oxide synthetically. low dimension and an analysis of its morphological characteristics. Due to its low cost, simple preparation, and industrial applicability, this approach possesses innovative qualities that are of major interest. In this study, the precipitation method is used to report the synthesis of CeO₂ nanoparticles, which are then calcined at 600°C. The CeO₂'s structural and symmetrical characteristics have been investigated via FTIR, XRD, and SEM studies. Group theory was used to identify the symmetrical, theoretical magnetism and magnetic nature of the nanoparticles.

Preparation of Cerium Oxide Nanoparticles

Cerium Sulphate 10g is dissolved in 80ml of 20% of Poly ethylene glycol &water (0.6g of PEG and 100ml of H₂O) .To this solution Sodium Bicarbonate 8g is dissolved in 100ml of Ethyl alcohol. The sample is prepared by using the Sonication method. (Ultra Sonicator) with a frequency of 6000mh and 80°C 120°C. The PEG is added for the extra effective and de-aggregation purpose. The precipitate is allowed to settle and separated and removing the impurities then dried at 100°C for 12 hrs then it is calcinated at 450°C for 15 Mins.

SAMPLE	PH VALUE		COLOR		VISCOSITY	
	Time	pH Value	Time	Color	Time	Viscosity
Cerium Oxide	30Mins	6	1 Hrs	Creamy Yellow	3Hrs	Liquid
	2Hrs	6-8	1Hrs	Slightly	3-9 Hrs	Colloidal
	6Hrs	8.5	30Mins	Brown	9-10Hrs	Gel
	10 Hrs	10	4Hrs	Brown		
	13 Hrs	11	9Hrs	Drak Brown	13 Hrs	Liquid and soild
			14Hrs	Mliky white		separated

X-RAY DIFFARACTION (XRD)

XRD is used as a fingerprint region for inorganic material used (crystal impact match 2 and diamond 3) software to draw structure. The blue line shows the observed data the red line shows matched data the colors represent for each match in the doped sample.

2 theta	d[Å]	hkl value	Reference 2theta forCeO ₂	Reference hkl for CeO ₂
28.556	3.1233	111	29.2	111
33.092	2.7049	002	33.1	200
47.500	1.9126	022	47.5	220
56.362	1.6311	113	57.6	311
59.110	1.5617	222	59.0	222
76.730	1.2411	133	76.7	331

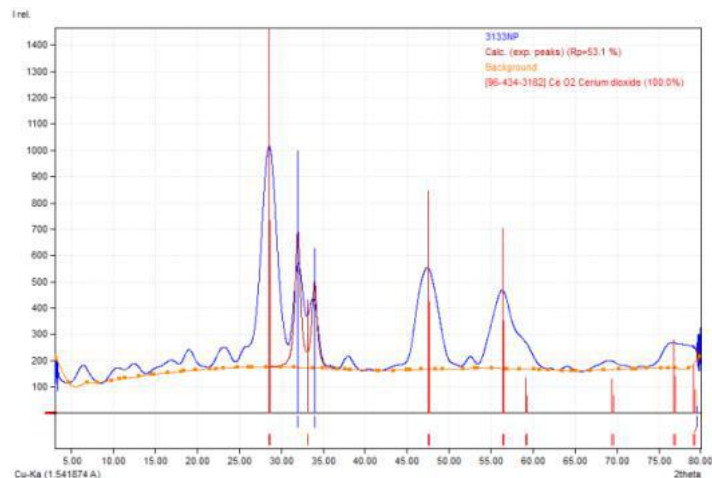


Fig-1 Smoothed Background Data for XRD

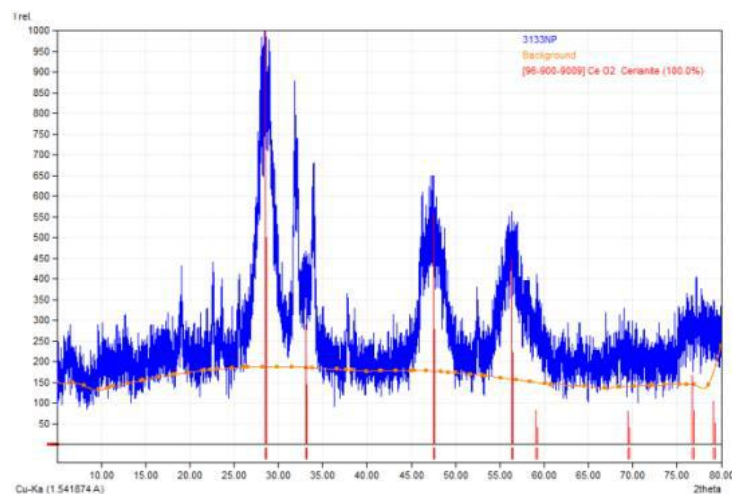


Fig-2 Original XRD Data

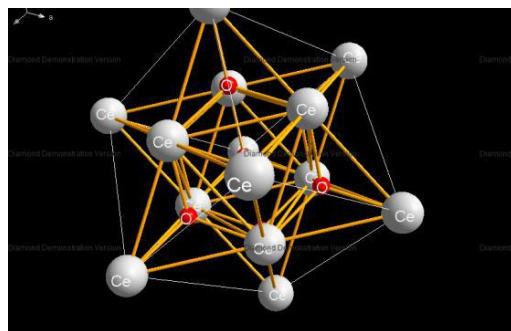


Fig-3(a)

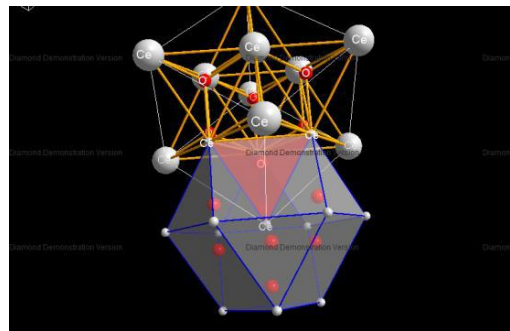


Fig-3(b)

Fig-3(a),Fig-3(b) Structure and magnetic symmetry of CeO₂ by diamond software

Effect of Doping

In our study we used CeO₂ were to study the magnetic nature of the sample by using group theory based computational method. The lattice arrangement of CeO₂ shows the cubic structures of the particles and the $f\bar{m}\bar{3}m$ space group and the atomic distance at 2.3422Å for Ce-O band. The XRD shows the high intensity and d-value at 3.1240Å this shows the sample is high purity (96-900-9009 ref data number). The atomic distance shows the practice is arranged in the perfect grain size and shape. The hkl value of the high- intensity peak with d-value as 3.1240 (111) and second high-intensity peak with have d-value as 1.9131, and hkl value as (022) the two hkl value shows the samples are in 99% purity and perfect arranged size according to the grain size the sample are formed less than 100nm that shows the in SEM report. The size of the unit cell is complete match with reference data.

Magnetic nature is studied through Magnetic Group Table, 1-, 2- and 3-Dimensional Magnetic Sub periodic Groups and Magnetic Space Groups Daniel B. Litvin., book from the symmetric calculation spins aligned within the (a) plane of the cubic unit cell, forming an angle Θ of 55(2)° with respect to the a axis. Releasing the constraints did not lead to any noticeable improvement in magnetic moment; all magnetic structures can be viewed as pseudo cubic arrangements of magnetic Ce⁺ cations with a G-type anti ferromagnetic structure.

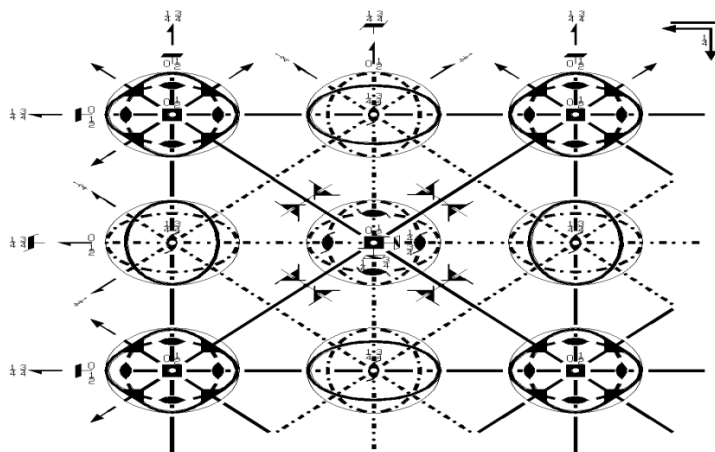


Fig-4 Magnetic Group Table for Fm3m Space Group

Table-3 Compatibility relations between the Brillouin zones for the space group $f\bar{m}3\bar{m}$ (225) of Paramagnetic CeO₂

$\Gamma(000)$									
Γ_1^+	Γ_2^+	Γ_2^-	Γ_1^-	Γ_3^+	Γ_3^-	Γ_4^+	Γ_5^+	Γ_4^-	Γ_5^-
Γ_1	Γ_2	Γ_1	Γ_2	$\Gamma_1 + \Gamma_2$	$\Gamma_1 + \Gamma_2$	$\Gamma_1 + 2\Gamma_2$	$2\Gamma_1 + \Gamma_2$	$2\Gamma_1 + \Gamma_2$	$\Gamma_1 + 2\Gamma_2$
$L(\frac{1}{2}\frac{1}{2}\frac{1}{2})$					$L'(00\frac{1}{2})$				
L_1^+	L_2^+	L_1^-	L_2^-	L_3^+	L_3^-	L_1^+	L_2^+	L_1^-	L_2^-
Γ_2	Γ_1	Γ_1	Γ_2	$\Gamma_1 + \Gamma_2$	$\Gamma_1 + \Gamma_2$	Z_2	Z_1	Z_1	Z_2
						$Z_1 + Z_2$			$Z_1 + Z_2$
$L''(\frac{1}{2}00)$					$\Lambda(\frac{1}{4}\frac{1}{4}\frac{1}{4})$			$R(\frac{1}{4}\frac{1}{4}\frac{3}{4})$	
L_1^+	L_2^+	L_1^-	L_2^-	L_3^+	L_3^-	Λ_1	Λ_2	Λ_3	R_1
V_1	V_1	V_1	V_1	$2V_1$	$2V_1$	$A_1 + A_2$	$A_1 + A_2$	$2A_1 + 2A_2$	$M_1 + M_2$
									$M_1 + M_2$
$X'(\frac{1}{2}\frac{1}{2}0)$									
X_1^+	X_2^+	X_3^+	X_4^+	X_5^+	X_1^-	X_2^-	X_3^-	X_4^-	X_5^-
Z_1	Z_2	Z_2	Z_1	$Z_1 + Z_2$	Z_2	Z_1	Z_1	Z_2	$Z_1 + Z_2$
$X''(0\frac{1}{2}\frac{1}{2})$									
X_1^+	X_2^+	X_3^+	X_4^+	X_5^+	X_1^-	X_2^-	X_3^-	X_4^-	X_5^-
V_1	V_1	V_1	V_1	$2V_1$	V_1	V_1	V_1	V_1	$2V_1$

- (i) The Brillouin zone for Cc (9) lies diagonally within the Brillouin zone for $f\bar{m}3\bar{m}$ (225).
- (ii) The upper rows list the representations of the little groups of the points of symmetry in the Brillouin zone for Fm3m and the lower rows list representations of the little groups of the related points of symmetry in the Brillouin zone for Cc. The representations in the same column are compatible in the following sense: Bloch functions that are basis functions of a representation Di in the upper row can be unitarily transformed into the basis functions of the representation given below Di.
- (iii) The notations of the representations are defined in Tables A3 and A2, respectively.
- (iv) Within the Brillouin zone for Fm3m the primed points are equivalent to the unprimed point.
- (v) The compatibility relations are determined by a C++ computer program in the way described in great detail in Ref. [27].

Scanning electron microscopy (SEM)

It's used to find the shape and size of the particle. The SEM image of the sample (CeO₂) shows of Fig (18) from the image it concluded out the morphology pure particles in a spherical shape, doped nanoparticles are formed spherical shape and size of the particle. The particles are formed in a spherical shape. The particle is not equally distributed. The size varies from 20-60nm. It may be due to environmental factors like far atmospheric moisture etc. From the image the average particle size is 20-60nm.

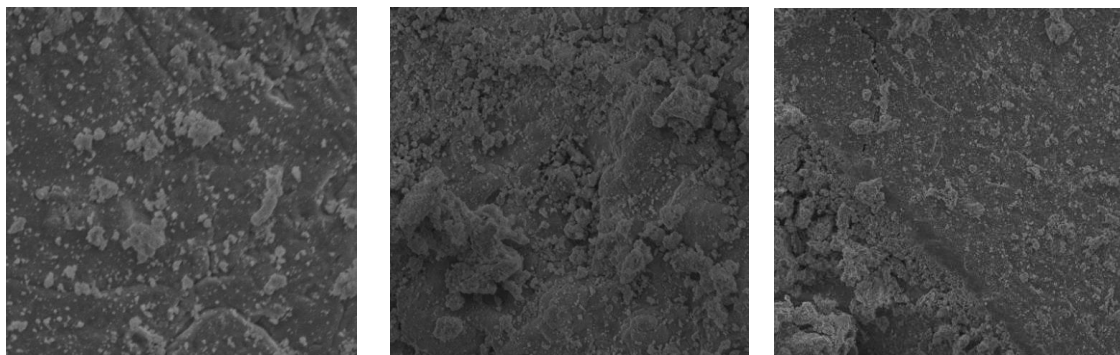


Fig-5 (a)

Fig-5(b)

Fig-5(c)

Fig-18(a), (b), (c) SEM image of the sample (CeO₂)

Effect of surfactant in size formation

We can often change the characteristics of suspension by understanding how individual colloids interact with one another. We may want to maximize the repulsive force between them to keep each particle discrete and prevent them from gathering into large, faster agglomerates. The attached counter ions in the solution form a layer and the charged atmosphere in the diffuse layer is referred to as the double layer. The thickness of the layer depends upon the type and concentrations of ions in solution (zeta potential). The double-layer formed to neutralize the charged colloid. When we use PEG as a surfactant it increases the viscosity of the solution the increasing viscosity decrease the interatomic colloidal particles. And increase the double layer thickness to this few presents of PEG to the solution medium reduce the surface tension of the solution medium and decrease the particle size.

Effect of doping

When the doping takes place, the impurity added to the parent material due to the impurity, the lattice arrangement of the parent material changed. When adding a known impurity to the parent material, the lattice disorder, takes place. It's due to lattice disorder. The morphology of the parent material was changed. In the present study, Fe and Mn used as a doping material and Mn oxide were used as the parent material. The atomic radius of Mn is higher than Fe, so the doping takes place in a good manner. The lower atomic radius gives the best result in doping and from lattice disorder this lattice disorder gives the change in morphology.

FOURIER TRANSFORM INFRARED SPECTROSCOPY (FTIR)

FTIR is used to identify the functional group of the prepared Nanoparticles. The sample shows absorption at 613cm⁻¹, 1103cm⁻¹ and 1330cm⁻¹ normally adsorption shows in 2800 - 3600cm⁻¹ is due to the removal of OH molecule. 613cm⁻¹ was assigned CeO Microcrystals and the position the peaks are dependent on the axial ratio (c/a) of the crystal. 1330cm⁻¹ was assigned for CeO bonding vibration mode lattice. Symmetrical stretching peaks confirm the presence of PEG in the sample which is used as a capping agent or surfactant, the doped material for the following peaks are assigned and confirmed the doping.

Table: FTIR Spectrum for Sample

Wavelength cm ⁻¹	Arrangement
613	stretching frequency of Ce-O
1330	“scissor” bending of H-O- is assigned to the Ce-O stretching mode.
1103	Vibrational modes of the CeO ₂ lattice.

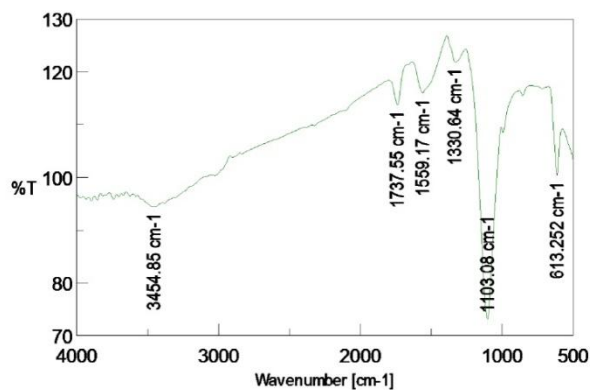


Fig -5 FTIR Spectrum for Sample

CONCLUSION

From overall report we concluded that the magnetism of cerium oxide was slightly changed to G-type anti ferromagnetic structure. This is due to the ultrasonic sound and we use PEG as a surfactant it increases the viscosity of the solution the increasing viscosity decrease the interatomic colloidal particles. And increase the double layer thickness to this few presents of PEG to the solution medium reduce the surface tension of the solution medium and decrease the particle size. This decreasing particle size leads to change in symmetrical change and it leads magnetic moment change.

REFERENCE

1. M. Farahmandjou, M. Zarinkamar and T.P. Firoozabadi Synthesis of Cerium Oxide (CeO₂) nanoparticles using simple CO-precipitation method, *Revista Mexicana de Física* 62 (2016) 496–499.
2. Sulochana S, Soundaravalli K, Selvan R. S. Effect of Aluminium, Magnesium Doping on Magnetic Nature of Zinc Oxide Nanoparticles Studied by X-Ray Diffraction Method. *Orient J Chem* 2022;38(3).
3. Ekkehard Krüger, Structural Distortion Stabilizing the Antiferromagnetic and Semiconducting Ground State of NiO, arXiv:1911.08190v1 [cond-mat.str-el] 19 Nov 2019.
4. Ekkehard Krüger Structural Distortion Stabilizing the Antiferromagnetic and Insulating Ground State of NiO, *Symmetry* 2020, 12, 56; doi:10.3390/sym12010056.

5. Ekkehard Krüger Structural Distortion Stabilizing the Antiferromagnetic and Semiconducting Ground State of BaMn₂As₂, arXiv:1607.05890v1 [cond-mat.str-el] 20 Jul 2016.
6. Ekkehard Krüger, Magnetic Structure of CoO, arXiv:2106.02577v2 [cond-mat.str-el] 25 Jul 2021.
7. Philipse AP, van Bruggen MP, Pathmamanoharan C: The preparation of magnetite nanoparticles for biomedical. Langmuir 1994, 10: 92. 10.1021/la00013a014
8. Garcell L, Morales MP, Andres-Verges M, Tartaj P, Serna CJ: a significant enhancement in the colloidal properties, such. J Colloid Interface Sci 1998, 205: 470. 10.1006/jcis.1998.5654
9. Cabuil V: Dekker Encyclopedia of Nanoscience and Nanotechnology, Chapter 119 Magnetic Nanoparticles:Preparation and Properties. Roldan group publications 2004.
10. Morcos SK: Nephrogenic systemic fibrosis following the administration of extracellular gadolinium based contrast agents: is the stability of the contrast agent molecule an important factor in the pathogenesis of this condition? Br J Radiol 2007, 80(950):73–76. 10.1259/bjr/17111243
11. Ersoy H, Rybicki FJ: Biochemical safety profiles of gadolinium-based extracellular contrast agents and nephrogenic systemic fibrosis. J Magn Reson Imaging 2007, 26(5):1190–1197. 10.1002/jmri.21135
12. Pita, M.; Tam, T.K.; Minko, S.; Katz, E. Dual magneto-biochemical logic control of electrochemical processes based on local interfacial pH changes. ACS Appl. Mater. Interfaces 2009, 1, 1166–1168. [CrossRef] [PubMed]
13. Jimenez, J.; Sheparovych, R.; Pita, M.; Narvaez Garcia, A.; Dominguez, E.; Minko, S.; Katz, E. Magneto-induced self-assembling of conductive nanowires for biosensor applications. J. Phys. Chem. C 2008, 112, 7337–7344.
14. Pita, M.; Abad, J.M.; Vaz-Dominguez, C.; Briones, C.; Mateo-Martí, E.; Martín-Gago, J.A.; del Puerto Morales, M.; Fernández, V.M. Synthesis of cobalt ferrite core/metallic shell nanoparticles for the development of a specific PNA/DNA biosensor. J. Colloid Interface Sci. 2008, 321, 484–492. [CrossRef] [PubMed]
15. Silva, S.M.; Tavallaie, R.; Alam, M.T.; Chuah, K.; Gooding, J.J. A comparison of differently synthesized gold-coated magnetic nanoparticles as ‘Dispersible Electrodes’. Electroanalysis 2016, 28, 431–438. [CrossRef]
16. Mandal, M.; Kundu, S.; Ghosh, S.K.; Panigrahi, S.; Sau, T.K.; Yusuf, S.M.; Pal, T. Magnetite nanoparticles with tunable gold or silver shell. J. Colloid Interface Sci. 2005, 286, 187–194. [CrossRef] [PubMed]

17. 56. Lim, J.K.; Majetich, S.A. Composite magnetic–plasmonic nanoparticles for biomedicine: Manipulation and imaging. *Nano Today* 2013, 8, 98–113. [CrossRef]
18. R. Shanmuga Selvan, and K. Gokulakrishnan. "Preparation and Characterization of Mn Doped γ -Fe₂O₃ Prepared by Self-Propagation Method." *International Journal of Applied Chemistry* 9.3 (2013): 291-297.
19. R. Shanmuga Selvan, and K. Gokulakrishnan. "Effect of Doping in Magnetic Character in γ -Fe₂O₃ Nano Particle." *Elixir Appl. Chem.* 103 (2017) 45526-45528.
20. Sulochana S, Soundaravalli K, Selvan R. S. Effect of Aluminium, Magnesium Doping on Magnetic Nature of Zinc Oxide Nanoparticles Studied by X-Ray Diffraction Method. *Orient J Chem* 2022;38(3). <http://dx.doi.org/10.13005/ojc/380310>